

## Observation of two-dimensional exciton-phonon quasibound states

N. T. Pelekanos, H. Haas, and N. Magnea

*Département de Recherche Fondamentale sur la Matière Condensée, CEA Grenoble, 17 rue des Martyrs, 38054 Grenoble Cedex 9, France*

V. I. Belitsky and A. Cantarero

*Department of Applied Physics, University of Valencia, 46100 Burjassot, Spain*

(Received 24 July 1997)

We demonstrate the existence of robust exciton-phonon quasibound states (EPQBS) in a two-dimensional semiconductor system, resulting from the binding of the  $e_1h_1$  and  $e_1h_2$  heavy-hole quantum-well excitons with an LO phonon. We show that increasing quantum confinement drastically weakens these two-dimensional EPQBS. A theoretical model including phonon confinement accounts qualitatively for our results. [S0163-1829(97)50140-8]

Phonon sidebands, situated about one LO phonon energy above an exciton line, have been observed as broad peaks in absorption spectra of bulk ionic insulators<sup>1,2</sup> (e.g., MgO) and polar semiconductors<sup>3</sup> (e.g., CdS), and were attributed to the exciton-LO phonon coupling via Fröhlich interaction which is strong in these materials. Qualitatively, it is possible to distinguish two different regimes by comparing the LO phonon energy  $\hbar\omega_0$  with the exciton binding energy  $E_B$  in a given compound. When  $E_B \gg \hbar\omega_0$  (e.g., alkali halides), the phonon sideband is centered at an energy distinctly above  $E_0 + \hbar\omega_0$ , where  $E_0$  is the energy of the exciton at  $\mathbf{q}=\mathbf{0}$ .<sup>2</sup> This behavior can be well accounted for by standard second-order perturbation theory for the indirect absorption process where an exciton with energy  $E_0(-\mathbf{q})$  and a phonon with energy  $\hbar\omega_0(\mathbf{q})$  are created simultaneously.

The situation becomes considerably more interesting and relevant to this work when  $E_B \sim \hbar\omega_0$ . In this case, there are pure electronic states, such as free electron-hole pairs, which are exactly or nearly degenerate with a free exciton+LO-phonon pair. This then allows a resonant Fröhlich coupling between the purely electronic and mixed exciton-phonon states, which under certain conditions may result in the formation of an exciton-phonon complex<sup>4</sup> with a finite binding energy  $\delta$ . The phonon sideband then occurs below  $E_0 + \hbar\omega_0$ , by an amount of energy  $\delta \approx 0.1\hbar\omega_0$ .

If the exciton-phonon complex overlaps with the electron-hole continuum, we distinguish it as an exciton-phonon quasibound state (EPQBS).<sup>5</sup> This is because EPQBS is intrinsically broadened by the resonant coupling to the continuum. In other words, the very same coupling that creates EPQBS automatically broadens it. This intrinsic broadening can be a good fraction of  $\hbar\omega_0$  in bulk systems,<sup>5</sup> accounting for the broad EPQBS lines observed experimentally.<sup>3</sup>

To our knowledge, EPQBS have never been observed in a two-dimensional (2D) system. We report here the observation and a comprehensive study of 2D EPQBS in CdTe/Cd<sub>1-x</sub>Zn<sub>x</sub>Te multiple quantum wells (MQWs), a 2D system with  $E_B \sim \hbar\omega_0$ .<sup>6</sup> We show that the 2D EPQBS, in contrast to their 3D counterparts, show up as sharp peaks in absorption spectra and exhibit a remarkable dependence on the heterostructure parameters.

The samples used in this study are listed in Table I along with the most important parameters. They typically contain 10 QW's and are grown coherently on transparent Cd<sub>0.88</sub>Zn<sub>0.12</sub>Te (100) substrates by molecular-beam epitaxy. For the electroabsorption experiments, semitransparent Schottky diodes were formed by standard processing.

In the lowest curve of Fig. 1, we show the zero electric field ( $E=0$ ) absorption spectrum at  $T=20$  K of sample A1 with well width  $L=125$  Å, barrier width  $L_b=125$  Å, and barrier Zn concentration  $x=10\%$ . Above the dominant  $e_1h_1$  QW exciton line (notice the  $\times 0.1$  scaling factor) a multitude of smaller peaks are clearly distinguished. Specifically, we observe the "forbidden"  $e_1h_2$  transition, the  $2s$  state of the  $e_1h_1$  exciton recognized by its large diamagnetic shift in a magnetic field perpendicular to the QW plane, and the  $e_1l_1$  line identified by its light holelike signature in polarized photoluminescence excitation (PPLE) spectra.<sup>7</sup> The upward arrows indicate the calculated energy positions of the same transitions and the agreement is very good. According to the same energy level calculation, there are no other excited states (such as  $e_1h_3$  or  $e_2h_1$ ) confined in the QW layer, owing to the small potential barrier heights in this sample

TABLE I. Experimental values of the oscillator strength  $f_1$  and binding energy  $\delta_1$  of the  $e_1h_1$ +LO EPBQS line, for different MQW samples of well width  $L$ , barrier width  $L_b$ , and barrier Zn concentration  $x$ .

Sample name	$L$ (Å)	$L_b$ (Å)	$x$ (%)	$f_1$ ( $\mu\text{eV}$ )	$\delta_1$ (meV)
A1	125	125	10	34	1.1
A2	130	130	26	5	0.25
A3	130	200	30.3	1	0
B1	157	94	21.5	48	3.2
B2	130	90	22	25	1.2
B3	85	86	21.9	0	0
C1	123	152	21.6	12	0.3

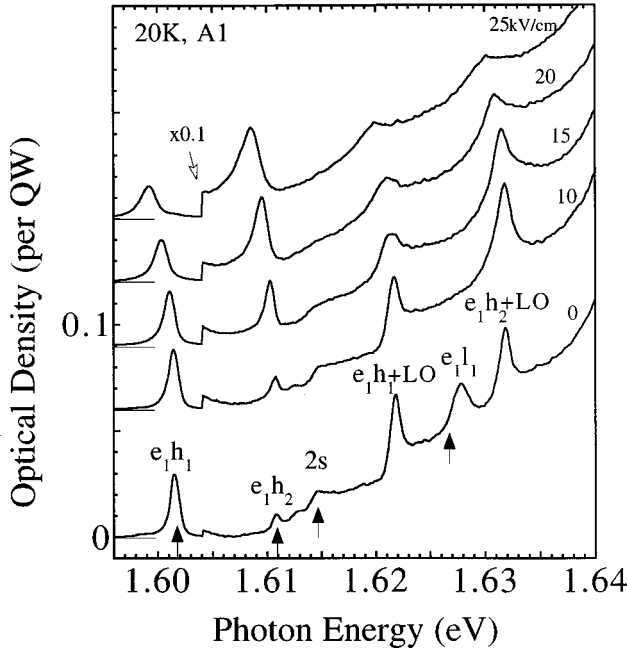


FIG. 1. Absorption spectra as a function of the electric field of sample A1 exhibiting pronounced EPQBS's, denoted as  $e_1h_1 + \text{LO}$  and  $e_1h_2 + \text{LO}$ . The upward arrows below the other identified QW transitions indicate their calculated positions.

(40 meV for the electrons and only 16 meV for the heavy holes). Nevertheless, two additional well-defined peaks remain in the spectrum and we identify them as the  $e_1h_1 + \text{LO}$  and the  $e_1h_2 + \text{LO}$  EPQBS.

The identification is justified as follows. First, the energy difference between  $e_1h_1 + \text{LO}$  and  $e_1h_1$  is 20.3 meV and between  $e_1h_2 + \text{LO}$  and  $e_1h_2$ , 21.1 meV, i.e., strikingly close to *but less* than  $\hbar\omega_0 = 21.45$  meV (Ref. 8)]. The small deviation from  $\hbar\omega_0$  corresponds well to the expected binding energy of the EPQBS, being here  $\delta_1 = 1.1$  meV for  $e_1h_1 + \text{LO}$  and  $\delta_2 = 0.3$  meV for  $e_1h_2 + \text{LO}$ . Second, as explained above, these lines cannot be assigned to an excited state confined in the QW. Third, we can exclude higher-order processes, such as resonant Raman scattering, since their contribution to absorption is negligible. Fourth, this assignment is consistent with the results of all the supplementary experiments we performed on this sample, in particular PPLE and transmission under perpendicular magnetic or electric field.<sup>7</sup>

As an example, in Fig. 1 we plot absorption curves with varying  $E$ . The quantum confined Stark effect in CdTe QW's is analyzed elsewhere.<sup>9</sup> Focusing now on the  $e_1h_1 + \text{LO}$  line, we observe that with increasing  $E$ ,  $e_1h_1 + \text{LO}$  redshifts, broadens and loses oscillator strength *at the same rate* as  $e_1h_1$ . This further supports its assignment. For instance, it excludes the possibility for  $e_1h_1 + \text{LO}$  to be instead an excited state weakly confined in the QW layer, because such a transition would be much more sensitive than  $e_1h_1$  to the field-induced band bending.

The fact that  $e_1h_2 + \text{LO}$  is of comparable intensity to  $e_1h_1 + \text{LO}$ , an exciton-phonon complex associated with a much stronger exciton, is at first sight puzzling. It can be understood, however, considering that the Fröhlich matrix element responsible for the EPQBS formation involves the transition between the ground exciton+LO phonon pair  $|0\rangle$

with in-plane wave vectors  $\mathbf{q}_{\text{ex}} = -\mathbf{q}_{\text{ph}} = \mathbf{q}$  and the free electron-hole pair  $|\mathbf{k}\rangle$  with in-plane wave vectors  $\mathbf{k}_e = -\mathbf{k}_h = \mathbf{k}$ . This can be written for a QW as<sup>10</sup>

$$\langle \mathbf{k} | H_F(\mathbf{q}) | 0 \rangle \propto C_q \left[ \frac{\varphi_e(\mathbf{q}, q_z)}{\left[ 1 + a_B^2 \left| \mathbf{k} - \frac{m_h}{M} \mathbf{q} \right|^2 \right]^{3/2}} - \frac{\varphi_h(\mathbf{q}, q_z)}{\left[ 1 + a_B^2 \left| \mathbf{k} + \frac{m_e}{M} \mathbf{q} \right|^2 \right]^{3/2}} \right], \quad (1)$$

where  $q_z$  is the size quantized component of the phonon wave vector,  $a_B$  is the 2D exciton Bohr radius,  $M = m_e + m_h$  the in-plane exciton mass, and  $C_q$  is the Fröhlich interaction. Given that  $C_q \propto 1/\sqrt{q^2 + q_z^2}$ , the role of phonons with small  $\mathbf{q}$  is dominant. For an ideal QW with infinitely high barriers and sufficiently narrow width ( $L \leq 2a_B$ ), the electron and hole wavefunctions for the  $e_1h_1$  exciton are identical along the  $z$  axis. The matrix elements  $\varphi_e(\mathbf{q}, q_z)$  and  $\varphi_h(\mathbf{q}, q_z)$  are then strictly equal, leading for  $\mathbf{q} \rightarrow \mathbf{0}$  to compensation of the electron and hole contributions in Eq. (1). This makes the Fröhlich interaction strictly forbidden in an ideal QW and is a result of exciton neutrality for large phonon wavelengths. Of course, in a real QW the electron and hole wavefunctions of  $e_1h_1$  penetrate differently into the barrier, and this dissymmetry results for  $\mathbf{q} \rightarrow \mathbf{0}$  to a finite decompensation in Eq. (1). We emphasize that decompensation is a necessary condition for strong resonant coupling between the electron-hole and exciton-phonon pairs and hence, for EPQBS formation. For  $e_1h_2$ , however, even in the case of an ideal QW there is always a large decompensation due to the different electron and hole wave functions. The larger decompensation for  $e_1h_2$  compared to  $e_1h_1$  can explain how  $e_1h_2 + \text{LO}$  is of comparable intensity to  $e_1h_1 + \text{LO}$ . It does not explain, however, why  $e_1h_2 + \text{LO}$  is also stronger than its zero-phonon associate  $e_1h_2$  exciton.

To shed light on this question we refer to the  $E$  dependence of  $e_1h_2 + \text{LO}$  and  $e_1h_2$ , as seen in Fig. 1. Both lines redshift identically, as expected. But what is unusual is that while  $e_1h_2$  gains oscillator strength as it becomes more dipole allowed in  $E$ ,  $e_1h_2 + \text{LO}$  loses strength after an initial increase. To explain this behavior, we suggest that the dominant mechanism in forming the  $e_1h_2 + \text{LO}$  state is resonant coupling of the  $e_1h_2 + \text{LO}$  phonon pair state to the continuum states, not of  $e_1h_2$ , but of the optically allowed  $e_1h_1$ . This hypothesis satisfies the decompensation condition discussed above and can explain why  $e_1h_2 + \text{LO}$  is stronger than  $e_1h_2$  at  $E=0$ .

Next we discuss the dependence of EPQBS on heterostructure parameters. In Table I, we list the binding energy  $\delta_1$  and oscillator strength  $f_1$  (defined as the spectrally integrated optical density per QW) for  $e_1h_1 + \text{LO}$  in various samples. The results for  $e_1h_2 + \text{LO}$  are similar with the exception of smaller  $\delta_2$ . Inspecting Table I, we conclude first that as  $f_1$  increases,  $\delta_1$  also increases. This is consistent with the EPQBS picture. Second, we conclude that increasing confinement drastically weakens the EPQBS. For instance, in

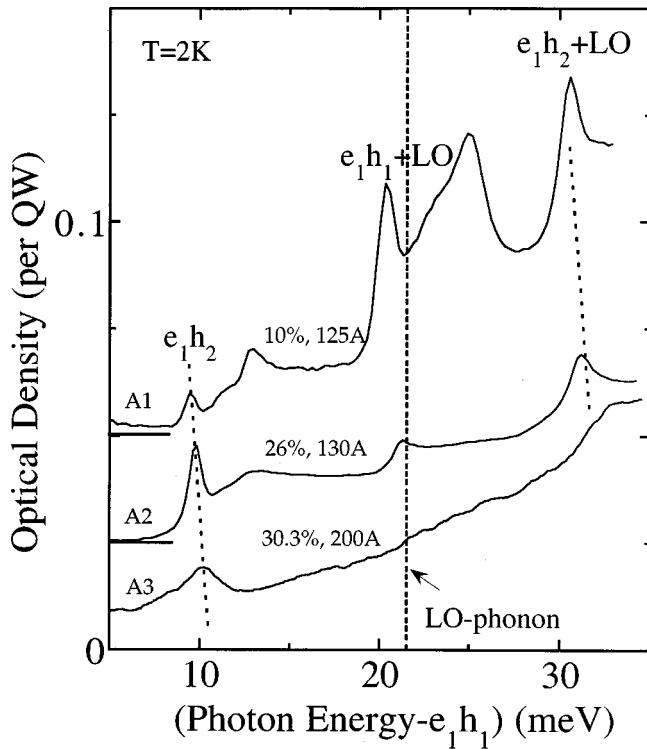


FIG. 2. EPQBS in samples with the same QW width but with barrier height and width increasing from top to bottom.

Fig. 2 we compare the optical density of the three samples of group A in Table I. They have practically the same  $L$  but the barrier height and width increases from top to bottom in the figure. Both  $e_1h_1+LO$  and  $e_1h_2+LO$  lines decrease strongly as the barrier becomes more confining. Notice the simultaneous decrease in  $\delta_1$  as the  $e_1h_1+LO$  peaks converge to the LO-phonon marker.

A similar strong dependence is observed for group B in Table I where  $L$  is varied but the barrier height and width are kept identical. In this group, the EPQBS is stronger for the wider QW's. A weaker dependence on barrier width is also deduced by comparing samples C1 and B2 in Table I, where  $L$  and  $x$  are constant but  $L_b$  is varied.

The quenching of EPQBS observed in Fig. 2 is quite striking, considering that these samples have practically the same small electronic confinement energies ( $L \approx 2a_B$ , with  $a_B = 70 \text{ \AA}$  in CdTe) and the same  $E_B$  ( $\approx 16 \text{ meV}$  for  $e_1h_1$ ). At first sight one could attribute the strong reduction of  $e_1h_1+LO$  to decreasing decompensation for  $e_1h_1$  as the barrier heights increase and we get closer to the ideal QW limit. This argument, however, cannot explain why  $e_1h_2+LO$  also decreases drastically, since for  $e_1h_2$  there is large decompensation even in an ideal QW. The simultaneous strong decrease of both  $e_1h_1+LO$  and  $e_1h_2+LO$  lines in samples where the electronic wave functions remain practically the same strongly indicates the key role of *phonon confinement* in understanding these 2D EPQBS.

Phonon confinement in MQWs results from the different LO phonon frequencies in the well and barrier layers. When the phonon gap is large (e.g., in GaAs/AlAs MQW's) the well phonon modes are localized in the QW with a quantized wave vector  $q_z = n\pi/L$  where  $n = 1, 2, \dots$ . In cases, however,

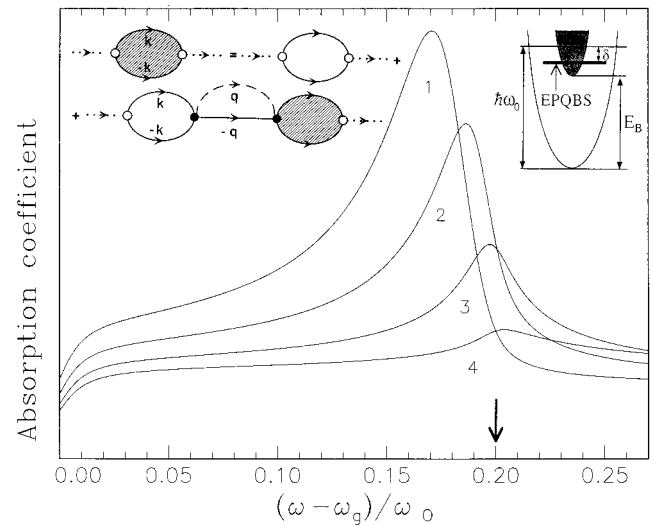


FIG. 3. Calculated absorption profiles for different phonon confinement factors  $q_z L_m$ . (1)  $q_z L_m = 0.05$ , (2) 0.1, (3) 0.2, (4) 0.4. The arrow indicates the  $E_0 + \hbar\omega_0$  threshold.

with a relatively small phonon gap ( $= 15 \text{ cm}^{-1}$  in GaAs/Ga<sub>0.6</sub>Al<sub>0.4</sub>As MQWs), the phonon modes are leaky, their extension larger than  $L$ , and the effective  $q_z$  smaller than  $\pi/L$ .<sup>12</sup> Clearly, all our samples are, to a varying degree, in this weak phonon confinement regime since the phonon gap never exceeds  $10 \text{ cm}^{-1}$ . More specifically, for sample A1 with  $x = 10\%$ , the phonon gap is merely  $3 \text{ cm}^{-1}$ ,<sup>13</sup> and the phonon mode may well extend over several periods of the structure. On the other hand, for sample A3 with  $x = 30\%$  and a much larger phonon gap ( $\approx 10 \text{ cm}^{-1}$ ) the phonon mode is better confined and its extension approaches  $L$ . We attribute the results of Fig. 2 (and of Table I) mainly to the different phonon confinement situations in the various samples. This seems to be supported by our theoretical model, that we describe next.

We calculated absorption profiles modifying the approach of Ref. 14 to the QW case and assuming phonon quantization along the  $z$  axis. We neglect interface phonons, as their contribution to EPQBS is negligible due to reduced overlap with the QW excitons. This is supported by our data on sample group B, showing that EPQBS is stronger for larger QW's for which the exciton-interface phonon overlap is smaller. We focus here on the case  $E_B \leq \hbar\omega_0$ , relevant to our samples. The corresponding energy dispersion graph is shown in the inset at top right of Fig. 3. In the inset at the top left of Fig. 3, we give the diagram representation of the Dyson equation for the absorption coefficient. For photons with energy  $\hbar\omega$  near  $E_0 + \hbar\omega_0$  and above the free electron-hole gap  $\hbar\omega_g$ , there is an optically active continuum of free electron-hole pairs with  $\mathbf{k}_e = -\mathbf{k}_h = \mathbf{k}$  (empty loop) each one of which can be degenerate with a pair state of a ground exciton (straight line) plus phonon (dashed line) with  $\mathbf{q}_{ex} = -\mathbf{q}_{ph} = \mathbf{q}$ , provided that  $(\hbar^2 q^2 / 2M) = (\hbar^2 k^2 / 2\mu) + (E_B - \hbar\omega_0)$  where  $\mu = m_e m_h / M$ . The direct electron-hole pair creation by the photon is followed by the infinite sequence of resonant or almost resonant Fröhlich transitions between the two types of pair states resulting in renormalization of the absorption (dashed loop). If the coupling is strong enough for  $\mathbf{q} \rightarrow \mathbf{0}$ , these resonating transitions may show up as an

EPQBS resonance at  $E_0 + \hbar\omega_0 - \delta$ , as we show next.

To analyze the absorption profile qualitatively, we approximate the large square brackets in Eq. (1) by a constant  $\xi$ .  $\xi$  can be viewed as the  $\mathbf{q} \rightarrow \mathbf{0}$  brackets limit and is a direct

measure of decompensation. The Dyson equation is then solved analytically and assuming a continuum of free electron-hole pairs and keeping only the 1s exciton contribution, the absorption coefficient is given by

$$\alpha(\omega) \sim \frac{[(q_z l_M)^2 + \eta]^2}{\left[ (q_z l_M)^2 + \eta - \beta \ln \frac{d - \epsilon}{\epsilon} \ln \frac{(q_z l_M)^2}{-\eta} \right]^2 + \beta^2 \pi^2 \left[ \ln \frac{(q_z l_M)^2}{-\eta} \right]^2}, \quad (2)$$

where  $\epsilon = (\omega - \omega_g)/\omega_0 > 0$ ,  $\eta = \epsilon - (\hbar\omega_0 - E_B)/\hbar\omega_0 < 0$ ,  $l_M = \sqrt{\hbar/(2M\omega_0)}$  is the polaron length for mass  $M$ ,  $d$  is a cutoff for  $\mathbf{k}$ , and  $\beta$  is an effective exciton-phonon coupling constant. A rough estimate of the latter is

$$\beta \sim \frac{\alpha_e l_{m_e}}{l_\mu} \frac{a_B a_B}{l_\mu X} \xi^2, \quad (3)$$

where  $\alpha_e \approx 0.3$  is the polaron constant for electrons in CdTe with  $\alpha_e l_{m_e} = \alpha_h l_{m_h}$ , and  $X$  is the extension of the phonon wave function along the  $z$  axis.

Aside from CdTe constants, Eq. (2) depends only on  $q_z l_M$ ,  $\beta$ , and the ratio  $E_B/\hbar\omega_0$ . In the range of parameters where the first term in the denominator becomes zero and the second one, which represents the intrinsic broadening, is small, the absorption shows a resonance. As an illustrative example, we plot in Fig. 3 the calculated profiles for different  $q_z l_M$  values and assuming  $E_B = 0.8\hbar\omega_0$  and  $\beta = 0.001$ . There are two important points to make: first, that the above model can reproduce a sharp EPQBS resonance below  $E_0 + \hbar\omega_0$ . We stress that this is a result of phonon quantization. Analyzing the case of interaction with bulk LO phonons we were unable to obtain strong EPQBS resonance even under assumption of decompensation. Second, that with increasing  $q_z l_M$  (i.e., increased phonon confinement) the resonance becomes weaker and the EPQBS binding energy  $\delta$  decreases, in agreement with experiment. On the other hand, for smaller  $q_z l_M$ ,  $\delta$  increases but at the same time the resonance broadens. Increasing the effective coupling constant  $\beta$  also has the same effect.

The small values of  $q_z l_M \approx 0.1$  for which we obtain a strong resonance correspond to a phonon extension larger than  $L$  and confirm that the weak phonon confinement present in our shallow MQW's is a favorable condition for EPQBS. However, the quantized character of phonons is still very important. It seems that a fine balance between the quantized character of phonons along with a rather small value of  $q_z$  is important for observing a strong EPQBS resonance.

Although we believe 2D EPQBS should be observable in other QW systems, the CdTe/(Cd,Zn)Te system has a concentration of a number of favorable conditions. First,  $E_B \sim \hbar\omega_0$ : in the samples used here  $E_B/\hbar\omega_0 \approx 0.75$ . Second, enhanced exciton-LO phonon coupling:  $\alpha_e$  is four times larger in CdTe than in GaAs. Third, we have large exciton oscillator strength and narrow linewidths, crucial for observing relatively weak transitions. Fourth, due to the large lattice mismatch between CdTe and ZnTe (7%), this heterostructure is typically grown with a small Zn content in the barrier, i.e., shallow.

In summary, we observed sharp EPQBS lines in a QW system. We show that, while size quantization of phonons is essential in creating strong 2D EPQBS, increased phonon confinement destroys them. Future work will address the dynamics of this fundamentally interesting 2D quasiparticle.

We thank R. Cox for a critical reading of the manuscript and V.I.B. thanks the European Union for financial support and the University of Valencia for its hospitality.

<sup>1</sup>W. Y. Liang and A. D. Yoffe, Phys. Rev. Lett. **20**, 59 (1968); W. C. Walker *et al.*, *ibid.* **20**, 847 (1968); R. Z. Bachrach and F. C. Brown, *ibid.* **21**, 685 (1968); H. Kanzaki and S. Sakuragi, J. Phys. Soc. Jpn. **27**, 109 (1969).

<sup>2</sup>G. Baldini *et al.*, Phys. Rev. Lett. **23**, 846 (1969).

<sup>3</sup>J. Dillinger *et al.*, Phys. Status Solidi **29**, 707 (1968).

<sup>4</sup>Y. Toyozawa and J. Hermanson, Phys. Rev. Lett. **21**, 1637 (1968); J. C. Hermanson, Phys. Rev. B **2**, 5043 (1970).

<sup>5</sup>Y. Toyozawa, in *Proceedings of the Third International Conference on Photoconductivity, Stamford, CA, 1969*, edited by Erik M. Pell (Pergamon, Oxford, 1971), p. 151.

<sup>6</sup>N. T. Pelekanos *et al.*, Appl. Phys. Lett. **61**, 3154 (1992).

<sup>7</sup>H. Haas, Ph.D thesis, Université Joseph Fourier de Grenoble, 1995.

<sup>8</sup>Slightly larger than  $\hbar\omega_0 = 21.3$  meV for bulk CdTe, owing to the 0.5% strain in the CdTe QW.

<sup>9</sup>H. Haas *et al.*, Phys. Rev. B **55**, 1563 (1997).

<sup>10</sup>C. Trallero-Giner and F. Comas, Phys. Rev. B **37**, 4583 (1988).

<sup>11</sup>B. Jusserand and M. Cardona, in *Light Scattering in Solids V*, Vol. 66 of *Topics in Applied Physics*, edited by M. Cardona and G. Güntherodt (Springer, Berlin, 1989), p. 49.

<sup>12</sup>D. S. Kim *et al.*, Phys. Rev. Lett. **68**, 1002 (1992).

<sup>13</sup>D. J. Olego *et al.*, Phys. Rev. B **33**, 3819 (1986).

<sup>14</sup>J. Sak, Phys. Rev. Lett. **25**, 1654 (1970).